Frontiers of Information Technology & Electronic Engineering
www.zju.edu.cn/jzus; engineering.cae.cn; www.springerlink.com
ISSN 2095-9184 (print); ISSN 2095-9230 (online)
E-mail: jzus@zju.edu.cn

Supplementary materials for

Yuanyang XUN, Siqi LI, Feiyu ZHANG, Yan HONG, Ke XU, Ligang CHEN, Song LIU, Bin LI, 2023. Rational design of semiconductor metal oxide nanomaterials for gas sensing by template-assisted synthesis: a survey. *Front Inform Technol Electron Eng*, 24(7):945-963. https://doi.org/10.1631/FITEE.2200552

1 Fundamentals of semiconductor metal oxide (SMO) gas sensors

1.1 Common detected gases

As hazardous substances or markers, many common gases need to be detectable in a timely manner by gas sensors. Such gases include CO (Naganaboina and Singh, 2021; Nami-Ana et al., 2021), NH_3 (Zhang Y et al., 2020; Wang D et al., 2021), NO_2 (Wang Z et al., 2017; Geng et al., 2021), H_2S (Kim DH et al., 2020; Chang et al., 2021), H_2 (Kim SM et al., 2018; Meng et al., 2022), ethanol (Ma et al., 2019; Sharma et al., 2021), HCHO (formaldehyde) (van den Broek et al., 2019; Jo et al., 2021), toluene (Ueda et al., 2020; Liu et al., 2022), acetone (Zhou T et al., 2021; Cai et al., 2022), xylene (Guo M et al., 2022; Li Y et al., 2022), n-butanol (Bai et al., 2019; Wang X et al., 2020; Guo W et al., 2022; Tian et al., 2022), trimethylamine (Chen Y et al., 2022; Li X et al., 2022), triethylamine (Yang L et al., 2022; Zhang S et al., 2023), and 3-hydroxy-2-butanone (Yang XY et al., 2022). Acetone can be used as a marker for disease pre-diagnosis of diabetic patients by detecting the acetone concentration in exhaled breath (Cho et al., 2021). It is vital to have a low acetone detection limit for gas sensors in the exhaled gas. For example, Hanh et al. (2021) prepared an acetone gas sensor based on Pt-Zn_2SnO_4 hollow octahedrals for exhaled-breath analysis in diabetes diagnosis. This sensor is of practical and scientific interest with an ultra-low detection limit of 1.276 ppb (1 ppb=1×10^{-9}). Yuan et al. (2020) synthesized novel CeO_2-WO_3 nanowires by hydrothermal and thermal decomposition processes for a micro-electromechanical system-based acetone gas sensor. The sensor has a response value of 1.3 to 500 ppb acetone and shows potential for use in screening exhaled breath for diabetes diagnosis. NO_2 is a hazardous gas with a pungent smell, and can cause serious harm to the environment and human health. Higher NO_2 concentrations adversely affect the respiratory tract including the throat, trachea, and lungs. Xie et al. (2021) designed a NO_2 gas sensor based on NiO-modified macroporous In_2O_3 thin film. The NO_2 sensor shows a high response value of 532.23 to 10 ppm NO_2 at 145 ℃. Wang Y et al. (2021) synthesized a polyoxometalate-modified Cu_2ZnSnS_4 nanoparticle based NO_2 sensor by a hydrothermal method, which shows excellent selectivity and long-term stability for NO_2. H_2S gas is produced in industrial production. It can damage human tissues, such as the nervous system and cardiovascular system. Qiao et al. (2020) prepared a H_2S sensor based on Mo-doped $BiVO_4$ polyhedrons with a fast response (8 s) by a two-step hydrothermal reaction and calcination. Wang C et al. (2020) designed a Co_2SnO_4-based H_2S sensor. The sensor has excellent reproducibility, outstanding selectivity, and a low detection limit, and can be used for monitoring halitosis disease. Ethanol is a widely prevalent organic solvent. Its detection is frequently used in breath analyzers, fermentation industries, food quality monitoring, and chemical industry biomedical and chemical process monitoring. Raghu et al. (2019) prepared carbon-doped anatase TiO_2 nanoparticles. This material can be used to create efficient ethanol sensors that operate at lower temperatures and have lower noise-to-signal ratios. Jiang et al. (2022) successfully synthesized ZnO hierarchical nanostructures self-assembled by a mesoporous nanosheet based ethanol sensor. The sensor responds clearly to 500 ppb ethanol, indicating a low ethanol detection limit. To sum up, gas sensors have strong application potential and

practical significance for gas detection. As a colorless and harmful gaseous organic amine, trimethylamine (TMA) is hazardous to the human skin, eyes, and respiratory tract. Chen W et al. (2018) designed a GO/Cu_2O nanocomposite TMA sensor that can detect TMA gas at less than 5 ppm. A sensor based on SnS/SnS_2 prepared by Zhou Q et al. (2022) shows good reversible selectivity and long-term stability, enabling the detection of TMA gas for industrial environment monitoring. Triethylamine (TEA) is a toxic and flammable gas that at concentrations of more than 10 ppm can have adverse effects on human health. A TEA sensor based on Zn_2SnO_4/SnO_2/ZnO and fabricated by a simple hydrothermal process has low cost and excellent performance (Sun et al., 2023). A TEA sensor with a typical hollow microfibrous structure designed by Zou et al. (2017) and manufactured using a sustainable biomass method results in an excellent response to TEA gas.

1.2 Performance parameters of SMO gas sensors

The performance parameters of gas sensors are important indexes to measure the sensing performance. Standard characteristic parameters include response, response/recovery time, selectivity, optimal operating temperature, repeatability, stability, and detection limit. According to the different properties of the gas and semiconductor to be measured, the response has different definitions. For example, when n-type semiconductors are exposed to reductive gas, the response is defined as the ratio of R_a (resistance of the sensor in air) to R_g (resistance of the sensor in the target gas). The response/recovery time is another important parameter of sensing performance, defined as the time required for the sensor to reach 90% of the total resistance change when the target gases are adsorbed/desorbed. Selectivity is defined as the sensor having a much higher response to a specific gas than to other gases being measured, and directly reflects the anti-interference ability of sensors in detection. The optimum operating temperature is the operating temperature when the gas sensitivity performance of the sensor reaches the optimum. The detection limit is the lowest effective gas concentration that a gas sensor can detect. Repeatability and stability indicate the detection stability of the gas sensor in a short time and a long time, respectively.

1.3 Profile of SMO gas sensors and sensing mechanisms

SMO gas sensors are devices that can detect various gases by turning their characteristics into measurable and effective electrical signals. The sensors can detect a wide variety of gases and have performance parameters, such as response, selectivity, and detection limit. They are simple and convenient to manipulate and can be used for qualitative and quantitative detection of gases.

Understanding the SMO sensing mechanism is crucial for designing efficacious semiconductor gas sensor nanomaterials. Oxidation and reduction reactions of gas on the semiconductor surface will lead to a change in the resistance value of the sensitive element. If the dissociation energy of the adsorbed gas molecules is higher than the semiconductor work function, the adsorbed gas will capture the electrons of the material and form the anion adsorber, namely the oxidizing gas; or if the energy is lower than the work function, the adsorbed gas will release the electrons to the material and form the cation adsorber, namely the reducing gas. For example, oxygen molecules are adsorbed on the surface when n-type semiconductors are exposed to ambient air. Then, the electrons will flow from n-type semiconductor to the oxygen molecules, forming surface-absorbed oxygen species (O^{2-} (ads), O^- (ads), O_2^- (ads)) and electron depleted regions. Thus, the resistance of the device is related to the content of the oxygen in the air. Next, the n-type semiconductor will be exposed to reductive gas. Immediately, the reductive gas molecules will readily react with adsorbed oxygen species, and the electrons will transfer from the gas to the conduction band, resulting in decreasing resistance (Fig. S1a). Therefore, the type and concentration of adsorbed gas can be measured on the basis of the resistance changes (Wang G et al., 2019b; Mnethu et al., 2020).

The process of gas sensing by a semiconductor device involves three main factors (Fig. S1b), including the transducer function, receptor function, and utility factor of the sensing body. Strategies such as doping (Zhao Q et al., 2015; Song et al., 2021), loading (Kondalkar et al., 2019; Ueda et al., 2021), and compositing (Li S et al., 2019; Zhou Y et al., 2021) usually are used to improve the transducer function. Carrier (electron or hole)

mobility can be enhanced by forming a Schottky junction, p–n heterojunction, or other junction systems. To enhance the receptor function, we can optimize the surface adsorption or reaction of the target gas by increasing the specific reaction (Zhang F et al., 2010; He et al., 2021), improving the catalytic effect (Hyodo et al., 2019; Zhao S et al., 2019), and adding a molecular sieve (Jo et al., 2021; Luo et al., 2021). The macroscopical expression of the utility factor includes the structure, morphology, and specific surface area (Chen R et al., 2020; Lee et al., 2020; Ng et al., 2020), which can be efficiently improved by template-assisted synthesis methods.

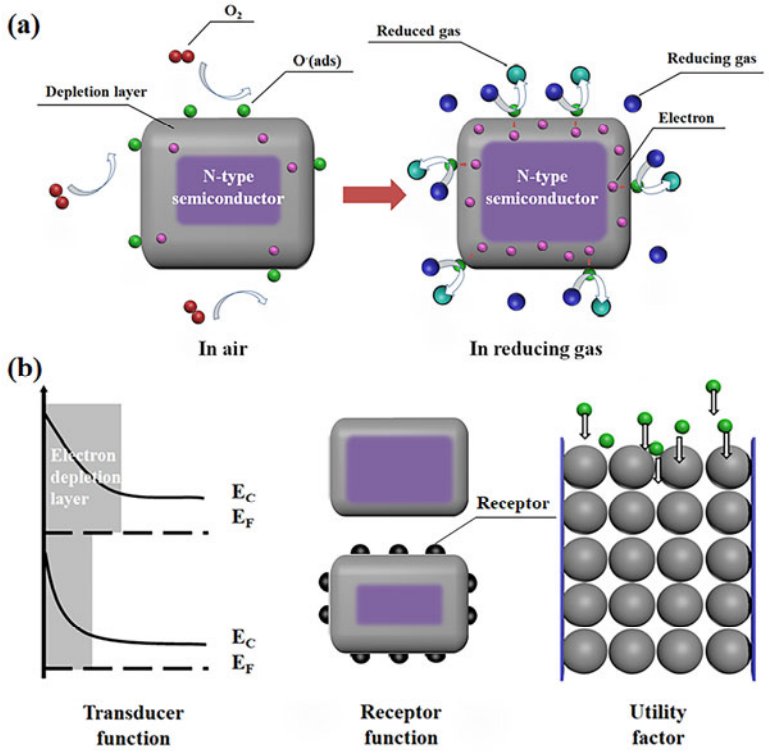

Fig. S1 Sensing mechanism: (a) schematic model of the reducing gas sensing mechanism of an n-type semiconductor; (b) schematic of the three main factors affecting gas sensing by a semiconductor device

2 Some main points in template-assisted synthesis

2.1 Categories of templates

In this review, we divided templates into two categories according to their source. One category requires a complex synthesis procedure, whereas the other is widely available and inexpensive. For example, carbon spheres and metal organic framework (MOF) templates need complicated synthesis methods, making them expensive. Their homogeneous morphology improves their competitiveness. On the other hand, some biomass templates are widely available, have a low cost, and require only simple treatment before use, attracting the interest of researchers. However, the irregular form and structure of biomass templates limits their gas sensing ability. Exploring the vastness of nature for high-performance and low-cost templates is thus the unwavering focus of our research.

2.2 Selection of synthesis methods

The choice of synthesis method is equally crucial in the template-assisted synthesis process. The electrospinning method (Sanger et al., 2018; Shin et al., 2021), deposition method (Sabri et al., 2018; Luong et al., 2021), hydrothermal method (Lai et al., 2018; Zheng et al., 2021), and dipping method (Li C et al., 2019; Teng

et al., 2020) are some of the most popular methods for preparing nanomaterials using a template-assisted synthesis process. We have loosely categorized the methods based on how materials of various dimensions are prepared. Electrostatic spinning is commonly used to make one-dimensional (1D) nanomaterials, whereas to make two-dimensional (2D) nanomaterials, a deposition process is often used. A dipping method can be used to make three-dimensional (3D) nanomaterials with simple components, while a hydrothermal method can be used when a sophisticated reaction process is required. Other synthesis methods such as the sol–gel method (Feng et al., 2021) and the spin coating method (Kwon et al., 2019), are also used to synthetize nanomaterials. A flexible technique selection is a requirement for a successful experiment.

In the process of template synthesis, we frequently use a hard or soft template. A hard template typically uses the inner or outer surface of the material as the framework, and the material is obtained by removing the framework. For example, Li W et al. (2015) fabricated a nanostructured polyaniline-based aromatic organic compound sensor using a single-walled carbon nanotube as a hard template. The structure of this material is extremely stable. Cao et al. (2020) used orange peel as a template and successfully prepared $FeYO_3$ microspheres. The template was removed by necessary calcination, and the material inherited the original shape of the template. At a working temperature of 330 °C, the sensor showed good sensing performance and distinct selectivity. Surfactant-based soft templates are micelles or inverse micelles. Ren et al. (2022) used block copolymers as a soft template and prepared a Si-WO_3-based gas sensor with a high specific surface area and abundant surface adsorbed oxygen species. The sensor exhibits excellent acetone sensing performance with a high response and selectivity. They also used block copolymers as a template to construct an unconventional Si-doped tungsten oxide nanowire array interweaved into 3D mesoporous superstructures with a large specific surface area. The Si-doped WO_3-based sensor exhibited excellent sensing performance to ethanol at 100 °C (Ren et al., 2021).

In contrast to these template methods, the self-template method is a concept that eliminates the need for a removal step and uses the precursor as a template for the synthesis of a porous catalytic structure (Wang G et al., 2018; Shen et al., 2021; Feng et al., 2022c; Hu et al., 2022). Recently, the self-template method has been used to prepare an increasing number of mesoporous materials with desirable composition and nanoarchitecture by transforming inorganic–organic hybrids at elevated temperatures under different atmospheric conditions. This synthesis strategy is a cost-effective and efficient method for preparing mesoporous metal oxide materials. Using the self-template method, Chen Y et al. (2022) developed a gas detecting material that can detect the freshness of seafood. In their research, metal-polyphenol hybrids were used as a precursor to prepare mesoporous Au-ZnO nanospheres. Based on the self-template method, Au species were evenly distributed on the mesoporous ZnO framework, significantly improving the sensing performance of the constituents. The developed gas sensor could also be used to monitor the spoilage process of fish. Using plant polyphenol as a ligand, Feng et al. (2022b) prepared a self-template synthesis of mesoporous Au-SnO_2 nanospheres for low-temperature detection of hazardous TEA. These nanospheres have a large pore size (5.1 nm) and a high specific surface area (86.5–105.2 m^2/g). The mesoporous Au-SnO_2 nanospheres have good selectivity and repeatability, a low detection limit (0.11 ppm) and a low working temperature (50 °C).

2.3 Selection of the calcination temperature

In addition to the complex synthesis process, the remaining details should not be ignored. The choice of appropriate parameters for the calcination process is very important in the template-assisted synthesis method. Calcination will affect the morphology and crystalline phase of the final product. To obtain good sensing materials, multiple experiments are required to determine an appropriate temperature. However, there is some regularity to follow. For example, the calcination temperature is usually 400–500 °C when a SiO_2 template is used (Kwon et al., 2019; Li C et al., 2019; Gao et al., 2020; Feng et al., 2021), 500–700 °C when an MOF template is used (Koo et al., 2018; Lai et al., 2018; Li H et al., 2020), and 350–550 °C when a polystyrene sphere template is used (Li C et al., 2019; Yi et al., 2019; Fei et al., 2020; Hung et al., 2020; Park et al., 2020). For other

templates such as plant tissues or absorbent cotton, the calcination temperature is usually above 500 ℃ (Zhang X et al., 2017; Sabri et al., 2018; Na et al., 2019; Teng et al., 2020; Zeng et al., 2020).

3 3D materials prepared using plant polyphenols as a template

Plant polyphenols are a common source of biomass that has low cost, no toxicity, potent metal chelation, and good adhesive properties toward a variety of substrates (Chen Z et al., 2013; Qin et al., 2021). These amorphous coordination polymers might substitute as a precursor to prepare a uniform porous structure material, which could be used as a template for tailoring the structure and creating SMO sensors. Studies of gas sensors based on semiconductor materials generated using plant polyphenols as a template are summarized in Table S1.

Table S1 Summary of nanomaterials for gas sensing using plant polyphenols as a template

Sensing material	Gas	Temperature	Concentration/Response	τ_{res} (s)	Reference
SnO_2	Ethanol	250 ℃	50 ppm/18.9	4	Feng et al. (2021)
Au-In_2O_3	Triethylamine	RT	10 ppm/54.9	101	Feng et al. (2022a)
Au-SnO_2	Triethylamine	50 ℃	5 ppm/5.16	37	Feng et al. (2022b)
Au-ZnO	Trimethylamine	250 ℃	10 ppm/52.6	12	Chen Y et al. (2022)
ZnO-Au	Ethanol	200 ℃	50 ppm/159	9	Lei et al. (2021)
ZnO	Ethanol	250 ℃	50 ppm/4.5	100	Wang G et al. (2018)

RT: room temperature; τ_{res}: response time. 1 ppm=1×10^{-6}

For example, tannic acid (TA) is a natural abundant polyphenol extracted from plant tissues (Wang G et al., 2019a; Lei et al., 2021;Feng et al., 2022a). Feng et al. (2021) used TA formaldehyde polymer as a template to prepare an ethanol sensor based on a nanoporous tin polyphenol formaldehyde polymer. The scanning electron microscope (SEM) image shows that the spherical morphology of SnO_2 is well-preserved after calcination (Fig. S2a). As shown in the transmission electron microscope (TEM) image (Fig. S2b), SnO_2 nanocrystals with a diameter of around 5–10 nm make up the mesoporous structure. The material has a uniform and porous structure with a large specific surface area of 185.6 m^2/g, ensuring good sensing performance. Fig. S2c shows the excellent response and repeatability of the sensor. Sometimes, adjusting the configurational distribution of catalysts can change the selectivity of a sensor. Again, using tannic acid as a template, Wang G et al. (2018) demonstrated a self-template strategy for the preparation of mesoporous SMO material by thermal decomposition of metal-phenolic coordination polymers. By altering the metal species, the mesoporous metal oxide spheres had either a solid or hollow inner structure. This material-based gas sensor can be used as a sensing platform for highly sensitive and selective detection of volatile organic compounds and biomolecules.

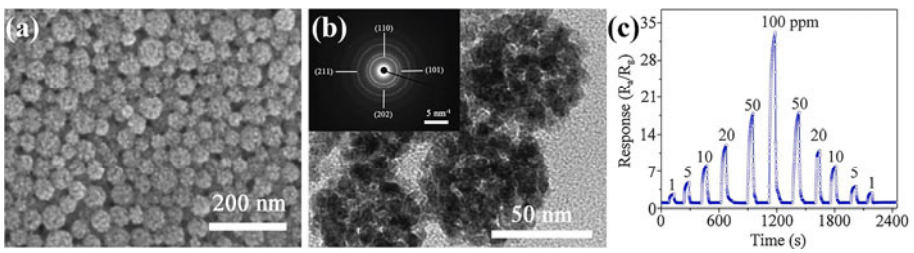

Fig. S2 Sample characterization: scanning electron microscope (SEM) (a) and transmission electron microscope (TEM) (b) images of mesoporous SnO_2 spheres; (c) response curves measured for different concentrations of ethanol (1 to 100 ppm) at 250 ℃

Reproduced from Feng et al. (2021), Copyright 2021, with permission from Elsevier. 1 ppm=1×10^{-6}

References

Bai J, Li Y, Liu Y, et al., 2019. $Au_{39}Rh_{61}$ alloy nanocrystal-decorated $W_{18}O_{49}$ for enhanced detection of n-butanol. *ACS Sens*, 4(10):2662-2670. https://doi.org/10.1021/acssensors.9b01073

Cai L, Dong X, Wu G, et al., 2022. Ultrasensitive acetone gas sensor can distinguish the diabetic state of people and its high performance analysis by first-principles calculation. *Sens Actuat B*, 351:130863. https://doi.org/10.1016/j.snb.2021.130863

Cao PF, Ma SY, Xu XL, et al., 2020. Preparation and characterization of a novel ethanol gas sensor based on $FeYO_3$ microspheres by using orange peels as bio-templates. *Vacuum*, 177:109359. https://doi.org/10.1016/j.vacuum.2020.109359

Chang J, Deng Z, Fang X, et al., 2021. Heterostructural $(Sr_{0.6}Bi_{0.305})_2Bi_2O_7$/ZnO for novel high-performance H_2S sensor operating at low temperature. *J Hazard Mater*, 414:125500. https://doi.org/10.1016/j.jhazmat.2021.125500

Chen R, Wang J, Luo S, et al., 2020. Unraveling photoexcited electron transfer pathway of oxygen vacancy-enriched ZnO/Pd hybrid toward visible light-enhanced methane detection at a relatively low temperature. *Appl Catal B*, 264:118554. https://doi.org/10.1016/j.apcatb.2019.118554

Chen W, Deng F, Xu M, et al., 2018. Go/Cu_2O nanocomposite based QCM gas sensor for trimethylamine detection under low concentrations. *Sens Actuat B*, 273:498-504. https://doi.org/10.1016/j.snb.2018.06.062

Chen Y, Li Y, Feng B, et al., 2022. Self-templated synthesis of mesoporous Au-ZnO nanospheres for seafood freshness detection. *Sens Actuat B*, 360:131662. https://doi.org/10.1016/j.snb.2022.131662

Chen Z, Wang C, Chen J, et al., 2013. Biocompatible, functional spheres based on oxidative coupling assembly of green tea polyphenols. *J Am Chem Soc*, 135(11):4179-4182. https://doi.org/10.1021/ja311374b

Cho CH, Choe YS, Oh JY, et al., 2021. Self-assembled 2D networks of metal oxide nanomaterials enabling sub-ppm level breathalyzers. *ACS Sens*, 6(9):3195-3203. https://doi.org/10.1021/acssensors.1c00367

Fei HF, Long Y, Yu HJ, et al., 2020. Bimodal mesoporous carbon spheres with small and ultra-large pores fabricated using amphiphilic brush block copolymer micelle templates. *ACS Appl Mater Interfaces*, 12(51):57322-57329. https://doi.org/10.1021/acsami.0c16566

Feng B, Feng Y, Qin J, et al., 2021. Self-template synthesis of spherical mesoporous tin dioxide from tin-polyphenol-formaldehyde polymers for conductometric ethanol gas sensing. *Sens Actuat B*, 341:129965. https://doi.org/10.1016/j.snb.2021.129965

Feng B, Wu Y, Chen Y, et al., 2022a. Polyphenol-mediated synthesis of mesoporous Au-In_2O_3 nanospheres for room-temperature detection of triethylamine. *ACS Appl Nano Mater*, 5(7):9688-9697. https://doi.org/10.1021/acsanm.2c01927

Feng B, Wu Y, Ren Y, et al., 2022b. Self-template synthesis of mesoporous Au-SnO_2 nanospheres for low-temperature detection of triethylamine vapor. *Sens Actuat B*, 356:131358. https://doi.org/10.1016/j.snb.2021.131358

Feng B, Feng Y, Li Y, et al., 2022c. Synthesis of mesoporous Ag_2O/SnO_2 nanospheres for selective sensing of formaldehyde at a low working temperature. *ACS Sens*, 7(12):3963-3972. https://doi.org/10.1021/acssensors.2c02232

Gao Z, Wang T, Li X, et al., 2020. Pd-decorated PdO hollow shells: a H_2-sensing system in which catalyst nanoparticle and semiconductor support are interconvertible. *ACS Appl Mater Interfaces*, 12(38):42971-42981. https://doi.org/10.1021/acsami.0c13137

Geng X, Li S, Mawella-Vithanage L, et al., 2021. Atomically dispersed Pb ionic sites in PbCdSe quantum dot gels enhance room-temperature NO_2 sensing. *Nat Commun*, 12(1):4895. https://doi.org/10.1038/s41467-021-25192-4

Guo M, Luo N, Chen Y, et al., 2022. Fast-response MEMS xylene gas sensor based on CuO/WO_3 hierarchical structure. *J Hazard Mater*, 429:127471. https://doi.org/10.1016/j.jhazmat.2021.127471

Guo W, Shuai Y, Liu X, et al., 2022. A n-butanol gas sensor with enhanced gas sensing performance based on Co-doped $BiVO_4$ polyhedrons. *Sens Actuat B*, 354:131221. https://doi.org/10.1016/j.snb.2021.131221

Hanh NH, Duy LV, Hung CM, et al., 2021. High-performance acetone gas sensor based on Pt-Zn_2SnO_4 hollow octahedra for diabetic diagnosis. *J Alloys Compd*, 886:161284. https://doi.org/10.1016/j.jallcom.2021.161284

He H, Zhao C, Xu J, et al., 2021. Exploiting free-standing p-CuO/n-TiO_2 nanochannels as a flexible gas sensor with high sensitivity for H_2S at room temperature. *ACS Sens*, 6(9):3387-3397. https://doi.org/10.1021/acssensors.1c01256

Hu J, Xiong X, Guan W, et al., 2022. Self-templated flower-like WO_3-In_2O_3 hollow microspheres for conductometric acetone sensors. *Sens Actuat B*, 361:131705. https://doi.org/10.1016/j.snb.2022.131705

Hung PS, Chou YS, Huang BH, et al., 2020. A vertically integrated ZnO-based hydrogen sensor with hierarchical bi-layered inverse opals. *Sens Actuat B*, 325:128779. https://doi.org/10.1016/j.snb.2020.128779

Hyodo T, Goto T, Takamori M, et al., 2019. Effects of Pt loading onto SnO_2 electrodes on CO-sensing properties and mechanism of potentiometric gas sensors utilizing an anion-conducting polymer electrolyte. *Sens Actuat B*, 300:127041. https://doi.org/10.1016/j.snb.2019.127041

Jiang B, Lu J, Han W, et al., 2022. Hierarchical mesoporous zinc oxide microspheres for ethanol gas sensor. *Sens Actuat B*, 357:131333. https://doi.org/10.1016/j.snb.2021.131333

Jo YK, Jeong SY, Moon YK, et al., 2021. Exclusive and ultrasensitive detection of formaldehyde at room temperature using a flexible and monolithic chemiresistive sensor. *Nat Commun*, 12(1):4955. https://doi.org/10.1038/s41467-021-25290-3

Kim DH, Cha JH, Lim JY, et al., 2020. Colorimetric dye-loaded nanofiber yarn: eye-readable and weavable gas sensing platform. *ACS Nano*, 14(12):16907-16918. https://doi.org/10.1021/acsnano.0c05916

Kim SM, Kim HJ, Jung HJ, et al., 2018. High-performance, transparent thin film hydrogen gas sensor using 2D electron gas at interface of oxide thin film heterostructure grown by atomic layer deposition. *Adv Funct Mater*, 29(7):1807760. https://doi.org/10.1002/adfm.201807760

Kondalkar VV, Duy LT, Seo H, et al., 2019. Nanohybrids of Pt-functionalized Al_2O_3/ZnO core-shell nanorods for high-performance MEMS-based acetylene gas sensor. *ACS Appl Mater Interfaces*, 11(29):25891-25900. https://doi.org/10.1021/acsami.9b06338

Koo WT, Cha JH, Jung JW, et al., 2018. Few-layered WS_2 nanoplates confined in Co, N-doped hollow carbon nanocages: abundant WS_2 edges for highly sensitive gas sensors. *Adv Funct Mater*, 28(36):1802575. https://doi.org/10.1002/adfm.201802575

Kwon KC, Suh JM, Lee TH, et al., 2019. SnS_2 nanograins on porous SiO_2 nnorods template for highly sensitive NO_2 sensor at room temperature with excellent recovery. *ACS Sens*, 4(3):678-686. https://doi.org/10.1021/acssensors.8b01526

Lai X, Cao K, Shen G, et al., 2018. Ordered mesoporous $NiFe_2O_4$ with ultrathin framework for low-ppb toluene sensing. *Sci Bull*, 63(3):187-193. https://doi.org/10.1016/j.scib.2018.01.015

Lee JE, Lim CK, Park HJ, et al., 2020. ZnO-CuO core-hollow cube nanostructures for highly sensitive acetone gas sensors at the ppb level. *ACS Appl Mater Interfaces*, 12(31):35688-35697. https://doi.org/10.1021/acsami.0c08593

Lei M, Gao M, Yang X, et al., 2021. Size-controlled au nanoparticles incorporating mesoporous ZnO for sensitive ethanol sensing. *ACS Appl Mater Interfaces*, 13(44):51933-51944. https://doi.org/10.1021/acsami.1c07322

Li C, Qiao X, Jian J, et al., 2019. Ordered porous $BiVO_4$ based gas sensors with high selectivity and fast-response towards H_2S. *Chem Eng J*, 375:121924. https://doi.org/10.1016/j.cej.2019.121924

Li H, Zhang N, Zhao X, et al., 2020. Modulation of TEA and methanol gas sensing by ion-exchange based on a sacrificial template 3D diamond-shaped MOF. *Sens Actuat B*, 315:128136. https://doi.org/10.1016/j.snb.2020.128136

Li S, Liu A, Yang Z, et al., 2019. Room temperature gas sensor based on tin dioxide@ polyaniline nanocomposite assembled on flexible substrate: ppb-level detection of NH_3. *Sens Actuat B*, 299:126970. https://doi.org/10.1016/j.snb.2019.126970

Li W, Guan P, Wei A, et al., 2015. Improving the gas sensing response of polyaniline via a porous carbon nanotube-based template. *Micro Nano Lett*, 10(4):206-208. https://doi.org/10.1049/mnl.2014.0638

Li X, Jin L, Ni A, et al., 2022. Tough and antifreezing MXene@Au hydrogel for low-temperature trimethylamine gas sensing. *ACS Appl Mater Interfaces*, 14(26):30182-30191. https://doi.org/10.1021/acsami.2c06749

Li Y, Wang H, Liu Y, et al., 2022. Bimetallic PtRu alloy nanocrystal-functionalized flower-like WO_3 for fast detection of xylene. *Sens Actuat B*, 351:130950. https://doi.org/10.1016/j.snb.2021.130950

Liu X, Duan X, Zhang C, et al., 2022. Improvement toluene detection of gas sensors based on flower-like porous indium oxide nanosheets. *J Alloys Compd*, 897:163222. https://doi.org/10.1016/j.jallcom.2021.163222

Luo S, Chen R, Wang J, et al., 2021. Designed synthesis of ZnO/Pd@ZIF-8 hybrid structure for highly sensitive and selective detection of methane in the presence of NO_2. *Sens Actuat B*, 344:130220. https://doi.org/10.1016/j.snb.2021.130220

Luong HM, Pham MT, Guin T, et al., 2021. Sub-second and ppm-level optical sensing of hydrogen using templated control of nano-hydride geometry and composition. *Nat Commun*, 12(1):2414. https://doi.org/10.1038/s41467-021-22697-w

Ma XH, Li HY, Kweon SH, et al., 2019. Highly sensitive and selective $PbTiO_3$ gas sensors with negligible humidity interference in ambient atmosphere. *ACS Appl Mater Interfaces*, 11(5):5240-5246. https://doi.org/10.1021/acsami.8b18428

Meng X, Bi M, Xiao Q, et al., 2022. Ultrasensitive gas sensor based on Pd/SnS_2/SnO_2 nanocomposites for rapid detection of H_2. *Sens Actuat B*, 359:131612. https://doi.org/10.1016/j.snb.2022.131612

Mnethu O, Nkosi SS, Kortidis I, et al., 2020. Ultra-sensitive and selective p-xylene gas sensor at low operating temperature utilizing Zn doped CuO nanoplatelets: Insignificant vestiges of oxygen vacancies. *J Colloid Interface Sci*, 576:364-375. https://doi.org/10.1016/j.jcis.2020.05.030

Na H, Zhang X, Deng Z, et al., 2019. Large-scale synthesis of hierarchically porous ZnO hollow tubule for fast response to ppb-level H_2S gas. *ACS Appl Mater Interfaces*, 11(12):11627-11635. https://doi.org/10.1021/acsami.9b00173

Naganaboina VR, Singh SG, 2021. Graphene-CeO_2 based flexible gas sensor: monitoring of low ppm CO gas with high selectivity at room temperature. *Appl Surf Sci*, 563:150272. https://doi.org/10.1016/j.apsusc.2021.150272

Nami-Ana SF, Nasresfahani S, Tashkhourian J, et al., 2021. Nanofibers of polyaniline and Cu(II)-L-aspartic acid for a room-temperature carbon monoxide gas sensor. *ACS Appl Mater Interfaces*, 13(33):39791-39805. https://doi.org/10.1021/acsami.1c07116

Ng S, Prasek J, Zazpe R, et al., 2020. Atomic layer deposition of SnO_2-coated anodic one-dimensional TiO_2 nanotube layers for low concentration NO_2 sensing. *ACS Appl Mater Interfaces*, 12(29):33386-33396. https://doi.org/10.1021/acsami.0c07791

Park SW, Jeong SY, Yoon JW, et al., 2020. General strategy for designing highly selective gas-sensing nanoreactors: Morphological control of SnO_2 hollow spheres and configurational tuning of Au catalysts. *ACS Appl Mater Interfaces*, 12(46): 51607-51615. https://doi.org/10.1021/acsami.0c13760

Qiao X, Xu Y, Yang K, et al., 2020. Mo doped $BiVO_4$ gas sensor with high sensitivity and selectivity towards H_2S. *Chem Eng J*, 395:5144. https://doi.org/10.1016/j.cej.2020.125144

Qin J, Liang G, Feng B, et al., 2021. Facile synthesis of metal-polyphenol-formaldehyde coordination polymer colloidal nanoparticles with sub-50 nm for T_1-weighted magnetic resonance imaging. *Chin Chem Lett*, 32(2):842-848. https://doi.org/10.1016/j.cclet.2020.05.021

Raghu AV, Karuppanan KK, Pullithadathil B, 2019. Controlled carbon doping in anatase TiO_2 (101) facets: superior trace-level ethanol gas sensor performance and adsorption kinetics. *Adv Mater Interfaces*, 6(4):1801714. https://doi.org/10.1002/admi.201801714

Ren Y, Xie W, Li Y, et al., 2021. Noble metal nanoparticles decorated metal oxide semiconducting nanowire arrays interwoven into 3D mesoporous superstructures for low-temperature gas sensing. *ACS Cent Sci*, 7(11):1885-1897. https://doi.org/10.1021/acscentsci.1c00912

Ren Y, Xie W, Li Y, et al., 2022. Dynamic coassembly of amphiphilic block copolymer and polyoxometalates in dual solvent systems: an efficient approach to heteroatom-doped semiconductor metal oxides with controllable nanostructures. *ACS Cent Sci*, 8(8):1196-1208. https://doi.org/10.1021/acscentsci.2c00784

Sabri YM, Kandjani AE, Rashid SSAAH, et al., 2018. Soot template TiO_2 fractals as a photoactive gas sensor for acetone detection. *Sens Actuat B*, 275:215-222. https://doi.org/10.1016/j.snb.2018.08.059

Sanger A, Kang SB, Jeong MH, et al., 2018. Morphology-controlled aluminum-doped Zinc oxide nanofibers for highly sensitive NO_2 sensors with full recovery at room temperature. *Adv Sci*, 5(9):1800816. https://doi.org/10.1002/advs.201800816

Sharma B, Karuppasamy K, Vikraman D, et al., 2021. Porous, 3D-hierarchical α-$NiMoO_4$ rectangular nanosheets for selective conductometric ethanol gas sensors. *Sens Actuat B*, 347:130615. https://doi.org/10.1016/j.snb.2021.130615

Shen J, Xu S, Zhao C, et al., 2021. Bimetallic Au@Pt nanocrystal sensitization mesoporous α-Fe_2O_3 hollow nanocubes for highly sensitive and rapid detection of fish freshness at low temperature. *ACS Appl Mater Interfaces*, 13(48):57597-57608. https://doi.org/10.1021/acsami.1c17695

Shin H, Kim DH, Jung W, et al., 2021. Surface activity-tuned metal oxide chemiresistor: toward direct and quantitative halitosis diagnosis. *ACS Nano*, 15(9):14207-14217. https://doi.org/10.1021/acsnano.1c01350

Song Z, Hu Z, Liu J, et al., 2021. Metastable antimony-doped SnO_2 quantum wires for ultrasensitive gas sensors. *Adv Electron Mater*, 8(5):2101049. https://doi.org/10.1002/aelm.202101049

Sun C, Liu H, Shao J, et al., 2023. Au-loaded Zn_2SnO_4/SnO_2/ZnO nanosheets for fast response and highly sensitive tea gas sensors. *Sens Actuat B*, 376:132951. https://doi.org/10.1016/j.snb.2022.132951

Teng Y, Zhang XF, Xu TT, et al., 2020. A spendable gas sensor with higher sensitivity and lowest detection limit towards H_2S: porous α-Fe_2O_3 hierarchical tubule derived from poplar branch. *Chem Eng J*, 392:123679. https://doi.org/10.1016/j.cej.2019.123679

Tian X, Yao L, Cui X, et al., 2022. Novel al-doped $CdIn_2O_4$ nanofibers based gas sensor for enhanced low-concentration n-butanol sensing. *Sens Actuat B*, 351:130946. https://doi.org/10.1016/j.snb.2021.130946

Ueda T, Defferriere T, Hyodo T, et al., 2020. Nanostructured Pr-doped Ceria (PCO) thin films as sensing electrodes in solid-electrolyte type gas sensors with enhanced toluene sensitivity. *Sens Actuat B*, 317:128037. https://doi.org/10.1016/j.snb.2020.128037

Ueda T, Boehme I, Hyodo T, et al., 2021. Effects of gas adsorption properties of an Au-loaded porous In_2O_3 sensor on NO_2-sensing properties. *ACS Sens*, 6(11):4019-4028. https://doi.org/10.1021/acssensors.1c01412

van den Broek J, Abegg S, Pratsinis SE, et al., 2019. Highly selective detection of methanol over ethanol by a handheld gas sensor. *Nat Commun*, 10(1):4220. https://doi.org/10.1038/s41467-019-12223-4

Wang C, Jiang L, Wang J, et al., 2020. Mixed potential type H_2S sensor based on stabilized zirconia and a Co_2SnO_4 sensing electrode for halitosis monitoring. *Sens Actuat B*, 321:128587. https://doi.org/10.1016/j.snb.2020.128587

Wang D, Zhang D, Yang Y, et al., 2021. Multifunctional latex/polytetrafluoroethylene-based triboelectric nanogenerator for self-powered organ-like MXene/metal-organic framework-derived CuO nanohybrid ammonia sensor. *ACS Nano*, 15(2): 2911-2919. https://doi.org/10.1021/acsnano.0c09015

Wang G, Qin J, Zhou X, et al., 2018. Self-template synthesis of mesoporous metal oxide spheres with metal-mediated inner architectures and superior sensing performance. *Adv Funct Mater*, 28(51):1806144. https://doi.org/10.1002/adfm.201806144

Wang G, Zhou X, Qin J, et al., 2019a. General synthesis of mixed semiconducting metal oxide hollow spheres with tunable compositions for low-temperature chemiresistive sensing. *ACS Appl Mater Interfaces*, 11(38):35060-35067. https://doi.org/10.1021/acsami.9b08694

Wang G, Fu Z, Wang T, et al., 2019b. A rational design of hollow nanocages Ag@CuO-TiO_2 for enhanced acetone sensing performance. *Sens Actuat B*, 295:70-78. https://doi.org/10.1016/j.snb.2019.05.075

Wang X, Liu F, Chen X, et al., 2020. In_2O_3 nanoparticles decorated ZnO hierarchical structures for n-butanol sensor. *ACS Appl Nano Mater*, 3(4):3295-3304. https://doi.org/10.1021/acsanm.0c00025

Wang Y, Fu X, Wang T, et al., 2021. Polyoxometalate electron acceptor incorporated improved properties of Cu_2ZnSnS_4-based room temperature NO_2 gas sensor. *Sens Actuat B*, 348:130683. https://doi.org/10.1016/j.snb.2021.130683

Wang Z, Huang L, Zhu X, et al., 2017. An ultrasensitive organic semiconductor NO_2 sensor based on crystalline TIPS-pentacene films. *Adv Mater*, 29(38):1703192. https://doi.org/10.1002/adma.201703192

Xie J, Liu X, Jing S, et al., 2021. Chemical and electronic modulation via atomic layer deposition of NiO on porous In_2O_3 films to boost NO_2 detection. *ACS Appl Mater Interfaces*, 13(33):39621-39632. https://doi.org/10.1021/acsami.1c11262

Yang L, Wang Y, Sui C, et al., 2022. Highly selective and humidity-resistant triethylamine sensors based on Pt and Cr_2O_3 nanoparticles. *ACS Appl Nano Mater*, 5(10):15053-15061. https://doi.org/10.1021/acsanm.2c03230

Yang XY, Shi YT, Gong FL, et al., 2022. Asymmetric interfacial oxygen sites of porous CeO_2-SnO_2 nanosheets enabling highly sensitive and selective detection of 3-hydroxy-2-butanone biomarkers. *Sens Actuat B*, 371:132500. https://doi.org/10.1016/j.snb.2022.132500

Yi SY, Song YG, Park JY, et al., 2019. Morphological evolution induced through a heterojunction of W-decorated NiO nanoigloos: synergistic effect on high-performance gas sensors. *ACS Appl Mater Interfaces*, 11(7):7529-7538. https://doi.org/10.1021/acsami.8b18678

Yuan K, Wang CY, Zhu LY, et al., 2020. Fabrication of a micro-electromechanical system-based acetone gas sensor using CeO_2 manodot-decorated WO_3 nanowires. *ACS Appl Mater Interfaces*, 12(12):14095-14104. https://doi.org/10.1021/acsami.9b18863

Zeng QR, Feng JT, Lin XC, et al., 2020. One-step facile synthesis of a NiO/ZnO biomorphic nanocomposite using a poplar tree leaf template to generate an enhanced gas sensing platform to detect n-butanol. *J Alloys Compd*, 815:150550. https://doi.org/10.1016/j.jallcom.2019.05.018

Zhang F, Zhu A, Luo Y, et al., 2010. CuO nanosheets for sensitive and selective determination of H_2S with high recovery ability. *J Phys Chem C*, 114(45):19214-19219. https://doi.org/10.1021/jp106098z

Zhang S, Song P, Wang Q, et al., 2023. Ultra-sensitive triethylamine gas sensor based on ZnO/MoO_3 heterostructures with ppb level detection. *Sens Actuat B*, 379:133239. https://doi.org/10.1016/j.snb.2022.133239

Zhang X, Dong Z, Liu S, et al., 2017. Maize straw-templated hierarchical porous ZnO: Ni with enhanced acetone gas sensing properties. *Sens Actuat B*, 243:1224-1230. https://doi.org/10.1016/j.snb.2016.12.076

Zhang Y, Zhang J, Jiang Y, et al., 2020. Ultrasensitive flexible NH_3 gas sensor based on polyaniline/$SrGe_4O_9$ nanocomposite with ppt-level detection ability at room temperature. *Sens Actuat B*, 319:128293. https://doi.org/10.1016/j.snb.2020.128293

Zhao Q, Ju D, Deng X, et al., 2015.Morphology-modulation of SnO_2 hierarchical architectures by Zn doping for glycol gas sensing and photocatalytic applications. *Sci Rep*, 5:7874. https://doi.org/10.1038/srep07874

Zhao S, Shen Y, Zhou P, et al., 2019. Design of Au@WO_3 core-shell structured nanospheres for ppb-level NO_2 sensing. *Sens Actuat B*, 282:917-926. https://doi.org/10.1016/j.snb.2018.11.142

Zheng Y, Wang L, Tian H, et al., 2021. Bimetal carbonaceous templates for multi-shelled $NiCo_2O_4$ hollow sphere with enhanced xylene detection. *Sens Actuat B*, 339:129862. https://doi.org/10.1016/j.snb.2021.129862

Zhou Q, Zheng C, Zhu L, et al., 2022. Tin sulfides heterostructure modified quartz crystal microbalance sensors with high sensitivity for hazardous trimethylamine gas. *Sens Actuat B*, 371:132520. https://doi.org/10.1016/j.snb.2022.132520

Zhou T, Dong W, Qiu Y, et al., 2021. Selectivity of a ZnO@ZIF-71@PDMS nanorod array gas sensor enhanced by coating a polymer selective separation membrane. *ACS Appl Mater Interfaces*, 13(45):54589-54596. https://doi.org/10.1021/acsami.1c16637

Zhou Y, Gu Q, Qiu T, et al., 2021. Ultrasensitive sensing of volatile organic compounds using a Cu-doped SnO_2-NiO p-n heterostructure that shows significant Raman enhancement. *Angew Chem Int Ed*, 60(50):26260-26267. https://doi.org/10.1002/anie.202112367

Zou Y, Chen S, Sun J, et al., 2017. Highly efficient gas sensor using a hollow SnO_2 microfiber for triethylamine detection. *ACS Sens*, 2(7):897-902. https://doi.org/10.1021/acssensors.7b00276